RSC Advances

This is an *Accepted Manuscript*, which has been through the Royal Society of Chemistry peer review process and has been accepted for publication.

Accepted Manuscripts are published online shortly after acceptance, before technical editing, formatting and proof reading. Using this free service, authors can make their results available to the community, in citable form, before we publish the edited article. This *Accepted Manuscript* will be replaced by the edited, formatted and paginated article as soon as this is available.

You can find more information about *Accepted Manuscripts* in the Information for Authors.

Please note that technical editing may introduce minor changes to the text and/or graphics, which may alter content. The journal's standard Terms & Conditions and the Ethical guidelines still apply. In no event shall the Royal Society of Chemistry be held responsible for any errors or omissions in this *Accepted Manuscript* or any consequences arising from the use of any information it contains.

ROYAL SOCIETY OF CHEMISTRY

www.rsc.org/advances

Close insights into the growth pattern of palladium nanocubes with controllable sizes

Jianzhou Wu[a], *Jing Zhao*[a], *Hehe Qian*[a], *Lei Yue*[b], *Yongsheng Guo*[a,*], *and Wenjun Fang*[a,*]

[a] Department of Chemistry, Zhejiang University, Hangzhou 310058, China

[b] Institute of Nuclear Physics and Chemistry, China Academy of Engineering Physics, Mianyang 621900, China

RSC Advances Accepted Manuscript

Abstract

Although shape and size controllable palladium nanocrystals have attracted enormous attention, the growth behavior of Pd nanocubes is not thoroughly estimated. In this work, the growth pattern of size controllable Pd nanocubes is studied systematically under varieties of reaction conditions. During the growth process of Pd nanocubes, various structures including concave cubes, triangular bipyramids, pentagonal bipyramids (decahedrons) and pentagonal rods can be generated due to disparate behavior of fresh Pd atoms. Different-sized nanocubes are prepared controllably through changing the dosage of KBr, which provides capping capacities toward {100} facets that cubes are enclosed with. Both ascorbic acid (AA) and KBr influence the reducing rate of Pd precursors and the growth kinetics of nanocrystals, and furthermore control the morphologies of products. These detailed researches supplement the understanding of crystal growth, and open up a close view toward the comprehending of atom movements in nanoscale.

Introduction

Shape and size controllable palladium nanocrystals (NCs) have shown great advantages in catalysis due to their specific facets,[1-5] and consequently have been widely investigated.[6-11] Palladium in nanoscale can appear in the morphologies of cubes, octahedrons, decahedrons, icosahedrons, rhombic dodecahedrons, as well as pentagonal rods and nanoplates.[12-21] Meanwhile, Pd nanocubes enclosed with {100} facets play a fundamental role in the formation of Pd-based core-shell architecture.[22-25] Although there have been some reports

RSC Advances Accepted Manuscript

describing the growth behavior of Pd nanocrystals,[6, 26-29] few concerns about the detailed growth pattern of Pd nanocubes.

Generally, the formation process of metal nanocrystals can be described with the LaMer's model,[26, 30] which divides the whole progress into three main periods, namely generation of atoms, self-nucleation and growth. It is uneasy to observe the generation of atoms and self-nucleation periods due to their extremely fast reaction rates,[26] while the growth period, a relatively slow process, can provide great quantities of information. For example, the facet development during the evolvement of platinum nanocubes has been discussed with density functional theory (DFT) calculations and in-situ transmission electron microscopy (TEM) observations,[31] while the oxidative etching phenomenon occurring throughout the formation of Pd cubes has been studied by decomposing the cubes with Br^- and H_2O.[32]

Pd nanocubes can be prepared through two main approaches, namely seed-mediated[33] or one-pot[12, 13] synthesis method. There have been some researches on the preparation of Pd nanocubes with bromide species.[4, 17] However, the relationships between the dosage of KBr, a capping agent towards Pd {100} facet, and the size of Pd nanocubes are not presented in detail. Close insights into the growth pattern of size controllable Pd nanocubes with KBr are demanded. In this work, we focus on the detailed results that turn out during the preparation of size-controllable palladium nanocubes. In combination with DFT calculations, close insights are engaged to clarify the growth mechanism, where Pd nanocubes are synthesized in

RSC Advances Accepted Manuscript

aqueous system under different conditions of reaction time, dosages of reducing and capping agents.

Experimental Section

Materials.

Potassium tetrachloropalladate (K_2PdCl_4, 99.95% metals basis), potassium tetrabromopalladate (K_2PdBr_4, Pd ≥ 20.5 %), ascorbic acid (AA, 99.99% metals basis), potassium bromide (KBr, 99.95% metals basis), polyvinylpyrrolidone (PVP, MW = 58000) potassium chloride (KCl, GR, 99.8 %) and potassium iodide (KI, ultra-pure, ≥ 99.5 %) were purchased from Aladdin Industrial Co., Shanghai, China. Acetone was obtained from Sinopharm Chemical Reagent Co., Ltd., China. All of these reagents were employed without further purification. Ultrapure water with resistivity above 1.82×10^5 Ω·m at 25 °C was produced from Millipore Q3 system.

Preparation of Pd Nanocrystals.

Herein, PVP, AA, and KBr were applied as stabilizer, reducing agent and capping agent, respectively. In a typical synthesis procedure, 278 mg of PVP, 163 mg of K_2PdCl_4 together with 1.5 g of KBr were dissolved in 15 mL of H_2O, pre-heated in a 100-mL flask at 85 °C for 5 minutes before adding 5 mL aqueous solution containing 150 mg of AA. Under this circumstance, the concentrations for PVP (calculated by monomer), K_2PdCl_4, KBr, and AA are 125, 25, 630, and 42.6 mmol/L, respectively. Afterwards, the reaction solution was kept stirred for 3 h, and then cooled down to room temperature. The products were collected by

RSC Advances Accepted Manuscript

diluting the resultant solution with acetone and centrifuged (5000 rpm, 10 min). The black precipitation was washed 5 times with water and acetone to remove excess PVP. Finally, the products were stored in a glass vessel with 10 mL of H_2O.

Characterization of Pd Nanocubes.

All of the samples were analyzed with TEM. During the procedure of sampling, 200 μL of particle aqueous suspension was mixed with 1 mL of ethanol to form a mixture with good volatility. A drop of the mixture was placed onto a copper grid coated with ultra-thin carbon film in atmosphere. Then the grid was dried in vacuum at 50 °C overnight. All the TEM images were obtained through HT7700 (Hitachi, Japan) with acceleration voltage at 100 kV, and the high resolution TEM (HRTEM) images were gained on JEM 2100F (JOEL, Japan) under 200 kV.

Results and Discussion

Shape Identification. Generally, two types of crystals can be generated, namely single and twinned crystals. To distinguish them, HRTEM analysis was employed with results exhibited in Fig. 1 and Fig. S1 of electronic supplementary information. Five different-shaped crystals, cube (concave cube included), decahedron, triangular bipyramid, pentagonal rod and icosahedron, can be observed.

RSC Advances Accepted Manuscript

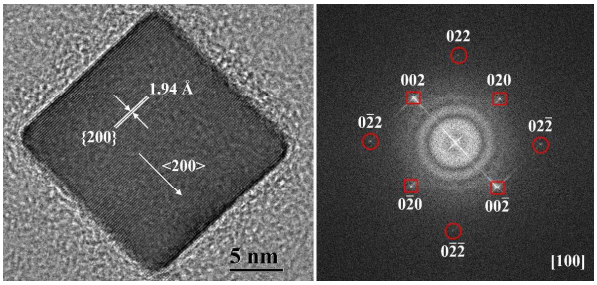

Fig. 1. HRTEM image of one Pd nanocube enclosed by {100} facets and the corresponding fast Fourier transformation (FFT) pattern.

Generation Process. The growth behavior of Pd nanocubes against reaction time was studied under typical synthesis procedure. The moment AA solution was added into the reaction system, the timer was started. At each reaction stage, 1 mL of reaction liquid was pipetted out and diluted with acetone to stop the growth progress at different reaction stages. We got reaction samples at 1, 2, 5, 10, 15, 20, 30, 45, 60, 90, 120 and 150 min with results presented in Fig. 2. According to the TEM images of these particles, the nucleation process could be divided within the beginning 5 min, and the crystal began to grow ever since. As shown in Fig. 2 (c ~ l), small spherical particles generated at early growth stages gradually evolved into cubes with the deposition of fresh Pd atoms onto particle surface, and consequently the crystal size increased. Particularly, as demonstrated in Scheme 1, the generated seeds would grow into primary cubes (or slightly truncated cubes) with three different kinds of explosive facets, namely {100} (capped with Br), {110} and {111} (atoms in green standing for {100} facets, while pink for {110} and yellow for {111}). Afterwards, fresh Pd atoms trended to deposit onto {111} facets (or corners) where surface energy was low[26] and atomic density was high, and progressively the atoms spread all over cube surfaces. Accordingly, we could name nanocubes as anisotropic growth products. After reacting for 90 min, the size of cubes

RSC Advances Accepted Manuscript

was stabilized at around 18 nm, indicating the accomplishment of the crystal growth. Thus, this growth course basically completed within 90 min under typical synthesis conditions, and was kept for another 1.5 h to carry through the progress entirely. Additionally, we undertook the reaction up to 10 h, but no apparent changes occurred (Fig. S2).

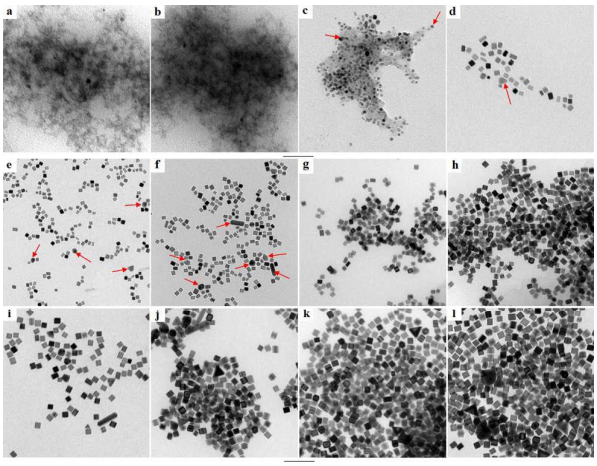

Fig. 2. TEM images of Pd NCs obtained at different reaction stages, from **a** to **l**: 1, 2, 5, 10, 15, 20, 30, 45, 60, 90, 120 and 150 min, sequentially (twinned crystals at early growth stages being pointed out with arrows). Scale bar: (**a** ~ **d**) 50 nm, (**e** ~ **l**) 100 nm.

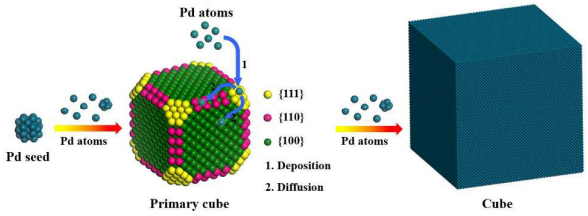

Scheme 1. Schematic illustration of the atom movements during the growth progress.

Dosage of KBr. Within shape-controlled growth process of metal nanomaterials, capping agents, such as PVP[34], citrate ions[18], metal ions[33] and halide ions[13], are usually required to manipulate the movements of fresh atoms. As one capping agent, KBr acts as a soft template leading Pd atoms to arrange along {100} direction orderly during the epitaxial growth of Pd

RSC Advances Accepted Manuscript

nanocubes.[35] Hence, the influence on Pd appearance from different amounts of KBr was studied. We conducted the experiments with 0, 188, 375, 750 and 1500 mg of KBr (the corresponding concentrations of KBr are 0, 78.8, 158, 315 and 630 mmol/L, respectively), respectively, and other conditions were kept the same as those in typical synthesis procedure. It could be clearly claimed that the crystal size increased as the portion of KBr enhanced, and in the meanwhile, the particles gradually evolved into cubes (Fig. 3). While KBr was replaced by KI or KCl with the same concentration under typical synthesis procedure, the cubes were no longer the major product (Fig. S3). Hence, we can confirm that KBr contributes greatly to the formation of nanocubes.

We measured the detailed data of those crystals in Fig. 3, including crystal average width/length or size, and calculated the average aspect ratio (Avg. L/W) (Fig. S4). Relating the average crystal width with KBr dosage, we find a linear correlation (Fig. 4). Indeed, $[PdBr_4]^{2-}$ is more stable than $[PdCl_4]^{2-}$,[36, 37] and thus tetrachloropalladte ions in water with the presence of Br^- will change into the form of $[PdCl_{4-n-m}Br_n(H_2O)_m]^{m-2}$ (equation 1). Afterwards, the hydrous precursor is gradually reduced into atoms by AA (equation 2).

$$[PdCl_4]^{2-} + n\ Br^- + m\ H_2O \rightleftharpoons [PdCl_{4-n-m}Br_n(H_2O)_m]^{m-2} + (n+m)\ Cl^- \quad (\mathbf{1})$$

$$[PdCl_{4-n-m}Br_n(H_2O)_m]^{m-2} + AA \rightarrow Pd^0 \quad (\mathbf{2})$$

Furthermore, different aqueous solutions with K_2PdCl_4 and KBr in contrast to that with K_2PdBr_4 were prepared and analyzed by UV-Vis (UV-2450, Shimadzu, Japan). As shown in Fig. 5a, the violet dash line is the signal of pure K_2PdBr_4 solution and the rest solid lines stand for the data of solutions consisting of Pd precursor and different amounts of KBr.

RSC Advances Accepted Manuscript

Obviously, Br^- coordinates to tetrapalladate. Characteristic absorption peaks of $[PdBr_4]^{2-}$ at 225 and 268 nm appear after the introduction of KBr and enhance as KBr dosage increases (Fig. 5b). The absorbance value is relevant with the interaction strength between Pd ion and ligand, which represents the stability of coordination compounds and the resistance ability toward reductant. Higher concentration of Br^- in reaction system causes greater absorbance value, and leads to relatively slower reducing rate and larger crystals.

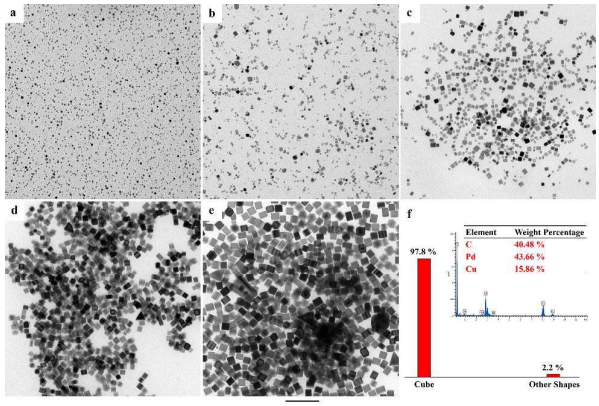

Fig. 3. (**a** ~ **e**) TEM images of Pd NCs gained with different dosages of KBr under typical synthesis procedure, the concentrations of KBr from **a** to **e**: 0, 78.8, 158, 315, and 630 mmol/L, respectively. Scale bar: 100 nm. (**f**) Percentage of cubes with other shapes and energy-dispersive X-ray spectroscopy (EDS) analysis of samples in **e**. Signals of C and Cu are caused by the copper grid.

RSC Advances Accepted Manuscript

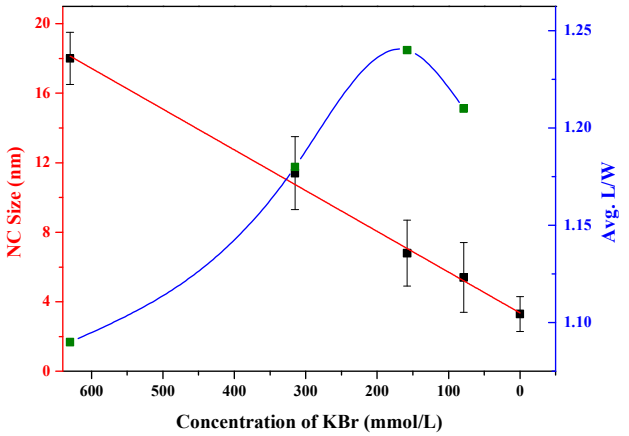

Fig. 4. The relationship between the size of nanocrystals and concentration of KBr, error bar showing size distribution of as-synthesized NCs. (■, size of nanocrystals, NC size; ○, average aspect ratio, Avg. *L/W*.)

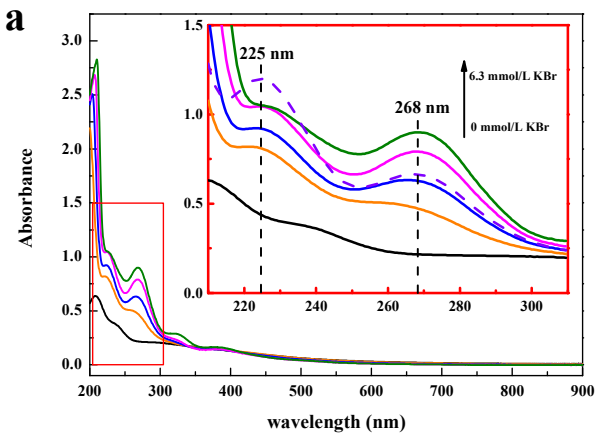

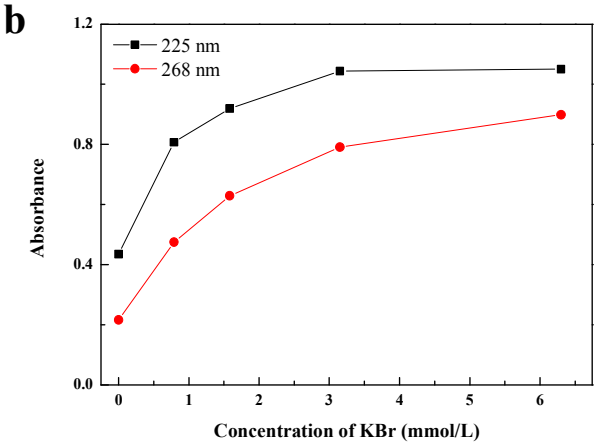

RSC Advances Accepted Manuscript

Fig. 5. (**a**) The UV-Vis spectra of aqueous solutions with 0.25 mmol/L K_2PdCl_4 and 0, 0.788, 1.58, 3.15, or 6.30 mmol/L KBr (solid lines) or 0.25 mmol/L K_2PdBr_4 (dash line). Insert: magnified spectra in red square. (**b**) The relationship between UV-Vis absorbance values at characteristic absorption peaks and KBr dosage.

However, when the concentration of Br^- in aqueous system was too low, it was still uneasy to obtain well-defined cubes because of the insufficient capping capacity. In the absence of KBr, it was not easy to gain well-defined cubes (Fig. S3c) when the same concentration of K_2PdBr_4 instead of K_2PdCl_4 was adopted under typical synthesis procedure. More Br^- was essential to smooth surface and build up clear structure. Under this circumstance, structures containing both {111} and {100} facets would be generated, for example, spheres and truncated cubes. On the contrary, high concentration of Br^- would lead to the formation of twinned structures, such as decahedrons and pentagonal rods. While the concentration of KBr was 630 mmol/L, some twinned structures appeared. At this point, the shape selection of cubes was over 95 % (Fig. 3 e). Afterwards, we attempted to increase the dosage of KBr up to 3 g, but the outcoming consisted of half cubes with average width at 17.6 nm and half twinned crystals (Fig. S5). The slightly attenuated cubic size might be owing to the strong coordinating ability of KBr towards Pd ions, which greatly slowed down the generation rate of fresh Pd atoms. Thus it influenced the self-nucleation period, leading to the formation of many twinned crystal seeds with {111} facets. During the growth period, fresh Pd atoms tended to deposit onto {111} facets where the electron density was higher (Scheme S1). Consequently, single crystal seeds could not obtain enough atoms to form

RSC Advances Accepted Manuscript

cubes as large as 18 nm. It could be concluded that within the KBr dosage range from from 0 to 630 mmol/L, we could simply control the addition amount of KBr to manipulate cubic dimension.

Dosage of AA. Reducing ability of reaction system is a key to controlling the growth pathway of crystals, influencing reaction kinetics, and furthermore determining product morphologies. As a reductant, AA possesses extraordinary reducing power that it can easily reduce some platinum group metal ions into bulk. The reduction ability of AA toward Pd precursor (taking $[PdCl_4]^{2-}$ form for instance) can be approximately calculated through electrochemical series. Under typical synthesis procedure, the reduction potential of AA can be given at 0.306 V (equation 3),[38] while the conditional reduction potential for $[PdCl_4]^{2-}$/Pd is 0.534 V (equation 4),

$$[AA_O]^- + 2H^+ + 2e \rightleftharpoons [AA_R]^- \qquad E'_{AA} = 0.306\ V \qquad (3)$$

$$PdCl_4^{2-} + 2e \rightleftharpoons Pd + 4Cl^- \qquad E'_{Pd} = 0.534\ V \qquad (4)$$

where $[AA_O]^-$ means AA in oxidative form, and $[AA_R]^-$ stand for its reductive form (detailed calculation in ESI). According to equation S1, while raising the initial concentration of AA, E'_{AA} will be enhanced, indicating the boost of reducing ability. The whole reaction process can be simplified as follows.

$$[PdCl_4]^{2-} + [AA_R]^- \rightleftharpoons Pd + 4Cl^- + [AA_O]^- + 2H^+ \qquad E' = 0.228\ V \qquad (5)$$

Apparently, this reaction is quite complete and its reaction rate is kinetically positively related to the dosage of AA.

RSC Advances Accepted Manuscript

Hence, we undertook typical synthesis procedure with different concentrations of AA: 21.3, 42.6, 85.2, 170 and 341 mol/L, respectively. As clearly displayed in Fig. 6, the crystals are enlarged with AA dosage enhanced, but change into slightly irregular hexahedrons with some defects or dislocations (Fig. 6e). According to the change tendency between NC size and AA dosage (Fig. 6f), there is a critical point where the crystals will no further expand even though the concentration of AA in reaction system increased. Before reaching the critical point, adequate Br^- supplies enough capping capacity for the dimensional growth of cubes, where the determination factor of cubic size is the dosage of AA. While the reducing ability in reaction system is superfluous, great quantities of Pd atoms can be generated within short time, leading to the formation of slightly irregular cubes with large size distribution. These crystals possess acute corners and curving surfaces, which are commonly called concave cubes[39]. Excess KBr should even decrease cubic dimension, which, together with the influence of AA, strongly proves that the size limitation of nanocubes prepared under typical synthesis procedure is approximately 20 nm.

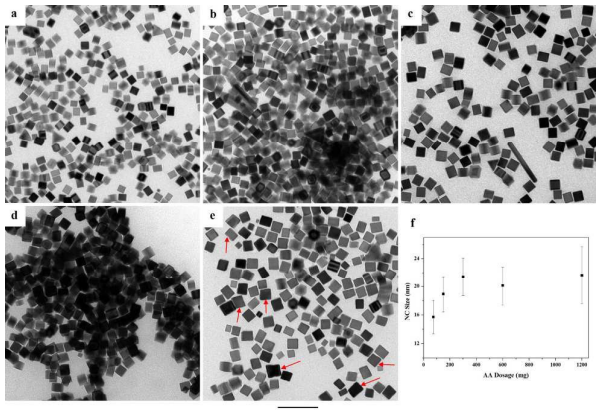

Fig. 6. (**a** ~ **e**) TEM images of Pd NCs achieved sequentially with 21.3, 42.6, 85.2, 170 and 341 mol/L of AA, respectively, under typical synthesis procedure. Some typical concave

RSC Advances Accepted Manuscript

cubes in sample **e** being pointed out with arrows. Scale bar: 100 nm. (**f**) The relationship between NC size and AA dosage.

Growth Behavior. As was stated, KBr owns outstanding capping ability toward {100} facet. According to primary DFT calculation (details in ESI), the electron density maps of three basic Pd facets exhibit three different types of electron-deficient regions (Scheme S1). Typically, {100} facets possess octahedral cavities where the electron density is low. Br^- tends to adsorb onto the octahedral cavities (Scheme S2) because of the attractive force of the holes. Coincidentally, the size of Br^- is 196 pm[40], which is close to the distance of Pd (200) faces (about 195 pm). Thus, we can draw the diagram describing the adsorption behavior of Br^- on Pd {100} facets in Scheme 2. Hence, the adsorption amount of Br^- on Pd nanocubes that every octahedral cavity of Pd surfaces is ideally capped with Br^- can be calculated with equation 5 (details in ESI),

$$\chi = \frac{N_{Br}}{N_{Pd}} = \frac{3\,a}{2\,n} \qquad (5)$$

where χ is the mole fraction Br^- in Pd cube, a is the lattice constant of Pd and n is the edge length of nanocube. Obviously, smaller cubes require more Br^- to form {100} facets. Indeed, the demand of Br^- to build cubes is far more than that just to cap the surfaces. Most of Br^- are engaged in the process of slowing down the reduction rate of Pd precursors (equations 1 and 2). Based on all evidence above, we can conclude the possible growth pattern of Pd nanocubes in Scheme 3. After the period of generation of atoms and self-nucleation, the primary cubes are generated and capped with Br^- on {100} facets. Sequentially, fresh Pd

RSC Advances Accepted Manuscript

atoms adsorb onto the surface of Br^- layer and gradually transpose onto Pd bulk. Eventually, the cubes grow into a well-defined crystal.

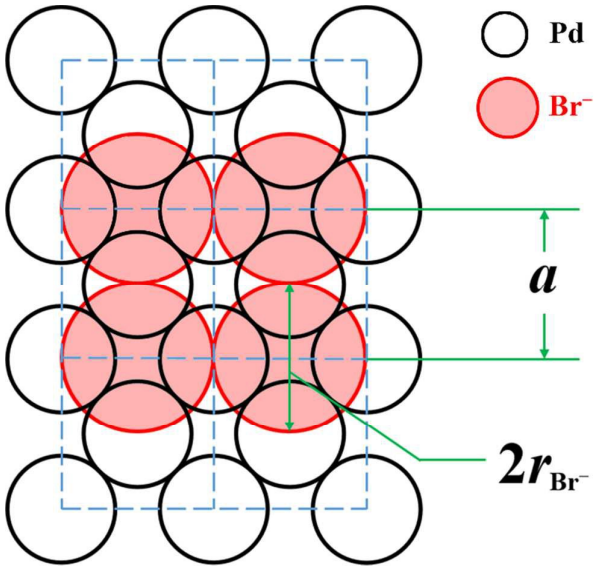

Scheme 2. Schematic diagram of bromide ions covering Pd {100} facet. The dash line means the unit cell of Pd.

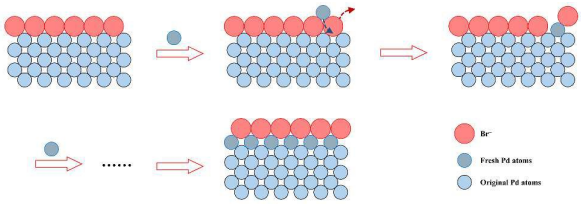

Scheme 3. Possible growth pathway of fresh Pd atoms onto Br-capped Pd {100} facet.

To thoroughly study the evolution progress during the formation of nanocubes, a series of comparative experiments were engaged. Representatively, 0.125 mmol K_2PdCl_4, 0.625 mmol PVP and certain amount of KBr were added into a reaction vessel, dissolved with water (< 5 mL) and preheated at 85 °C. Afterwards, a potion of AA solution was pipetted into the reaction system. Finally, 5 mL of reaction aqueous system was formed and heated for 3 h.

RSC Advances Accepted Manuscript

The concentrations for K_2PdCl_4 and PVP were the same as those in typical synthesis procedure. The concentrations of KBr and AA were listed in Table S1, and relevant TEM images were presented in Fig. S6. With the enhancement of KBr in reaction system, morphologies of the nanostructures are progressively regulated. However, when KBr dosage increases over certain amount, great quantities of twinned crystals turn up and cubes gradually disappear. With the participant of KBr, when the AA concentration in reaction system escalates, cubes will be enlarged before twinned crystals instead of cubes come out.

The phenomena above can be explained with the deposition and diffusion behavior of newly formed Pd atoms.[41] Typically in our reaction system, the deposition rate is mainly influenced by the generation rate of fresh Pd atoms, and the diffusion rate is majorly controlled by the transposition ability of fresh Pd atoms which is thermo-dependent. AA as well as KBr possesses abilities to determine growth results. Thermodynamically, structures enclosed with {100} facets are not thermostable enough, and cubes will evolve into crystals surrounded by {111} facets under high temperature.[12] During a synthesis procedure, when the dosage of AA is low, namely the diffusion rate of Pd atoms over seed surface overwhelming deposition rate, insufficient fresh Pd atoms restrict crystals at relative small sizes with truncated corners. While concentration of AA in reaction system is enhanced to the point where the atomic diffusion rate is substantially equal to deposition rate, the generation rate of Pd atoms analogously increases, inducing the formation of complete cubes. However, overdosed AA should accelerate the generation speed of Pd atoms excessively, in other words, that the diffusion rate is too slow to smooth crystal surfaces, causing defects or dislocations, and leading to the appearance of concave cubes and eventually twinned structures including

RSC Advances Accepted Manuscript

decahedrons and icosahedrons. On the other hand, Br^- coordinates with Pd^{2+} forming hydrous compounds, indirectly influencing the reducing rate. When more Br^- participates in the reaction, the reduction rate of Pd precursor is slower. However, overdosed Br^- limits the growth of cubes and encourages the formation of {111} facets due to the extreme slow generation rate of fresh Pd atoms. Consequently, large quantity of Br^- protects twinned structures and promotes the growth of pentagonal rods by capping the side facets. Hence, the appearance of twinned structures is mainly owing to the overdosed AA and KBr.

Eventually, we summarize the growth pattern of Pd nanocubes in Scheme 4. After converting from Pd precursor into seeds, PVP stabilized nanostructures transform into cubes, concave cubes, triangular bipyramids, decahedrons, pentagonal rods and other twinned crystals enclosed with {111} facets.

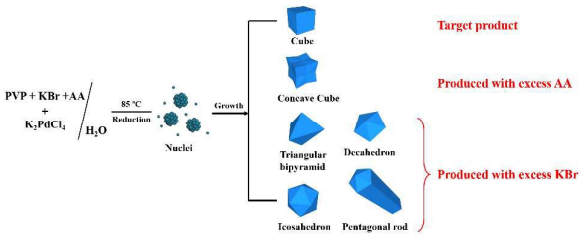

Scheme 4. Schematic illustration of the growth of Pd nanocubes with probable resultant morphologies.

Conclusion

Size-controllable nanocubes have been prepared with typical synthesis procedure, where K_2PdCl_4, PVP, AA, and KBr act as precursor, stabilizer, reductant and capping agent,

RSC Advances Accepted Manuscript

respectively. We have obtained nanocubes sized from 6 to 18 nm facilely by adjusting the dosage of KBr. This work gives a close view into the growth period of Pd nanocubes. Whether for AA or KBr, the influence toward cubic sizes and morphologies is indeed contributed through manipulating the formation rate of fresh Pd atoms. The detailed growth pathway of Pd nanocubes can help to understand the nature of shape selection under different situations. It also provides a promising way toward the generation of twinned crystals, including triangular bipyramids, decahedrons and pentagonal rods.

ASSOCIATED CONTENT

Footnote. Electronic Supplementary Information (ESI) available: calculation of electrochemical details for typical synthesis procedure, DFT calculation details, HRTEM images of different shapes, TEM images of Pd nanocubes and relative data. See DOI: 10.1039/x0xx00000x

Corresponding Author

*E-mail: fwjun@zju.edu.cn (W. Fang); wjjw@zju.edu.cn (Y. Guo). Tel: +86 571 88981416. Fax: +86-571-88981416.

NOTE

The authors declare no competing financial interest.

ACKNOWLEDGMENT

This work was supported by the National Natural Science Foundation of China (Nos. 21273201, J1210042).

RSC Advances Accepted Manuscript

REFERENCES

1. Q. Zhang, J. Xu, D. Yan, S. Li, J. Lu, X. Cao and B. Wang, *Catal. Sci. Technol.*, 2013, 3, 2016-2024.

2. Y. Han, Z. He, S. Wang, W. Li and J. Zhang, *Catal. Sci. Technol.*, 2015, 5, 2630-2639.

3. X. Zhang, H. Yin, J. Wang, L. Chang, Y. Gao, W. Liu and Z. Tang, *Nanoscale*, 2013, 5, 8392-8397.

4. S. Sreedhala, V. Sudheeshkumar and C. Vinod, *Nanoscale*, 2014, 6, 7496-7502.

5. M. Crespo-Quesada, A. Yarulin, M. Jin, Y. Xia and L. Kiwi-Minsker, *J. Am. Chem. Soc.*, 2011, 133, 12787-12794.

6. G. Berhault, M. Bausach, L. Bisson, L. Becerra, C. Thomazeau and D. Uzio, *J. Phys. Chem. C*, 2007, 111, 5915-5925.

7. L. Polavarapu, S. Mourdikoudis, I. Pastoriza-Santos and J. Perez-Juste, *CrystEngComm*, 2015, 17, 3727-3762.

8. M. Moreno, F. J. Ibanez, J. B. Jasinski and F. P. Zamborini, *J. Am. Chem. Soc.*, 2011, 133, 4389-4397.

9. C. F. Barnard, *Organometallics*, 2008, 27, 5402-5422.

10. J. E. Choe, M. S. Ahmed and S. Jeon, *J. Power Sources*, 2015, 281, 211-218.

11. A. A. Ensafi, M. Jafari-Asl, B. Rezaei, M. M. Abarghoui and H. Farrokhpour, *J. Power Sources*, 2015, 282, 452-461.

12. B. Lim, H. Kobayashi, P. H. C. Camargo, L. F. Allard, J. Y. Liu and Y. N. Xia, *Nano Res.*, 2010, 3, 180-188.

13. M. Jin, H. Liu, H. Zhang, Z. Xie, J. Liu and Y. Xia, *Nano Res.*, 2011, 4, 83-91.

RSC Advances Accepted Manuscript

14. X. Xia, S.-I. Choi, J. A. Herron, N. Lu, J. Scaranto, H.-C. Peng, J. Wang, M. Mavrikakis, M. J. Kim and Y. Xia, *J. Am. Chem. Soc.*, 2013, 135, 15706-15709.

15. Y. Xiong, I. Washio, J. Chen, H. Cai, Z.-Y. Li and Y. Xia, *Langmuir*, 2006, 22, 8563-8570.

16. Y.-H. Chen, H.-H. Hung and M. H. Huang, *J. Am. Chem. Soc.*, 2009, 131, 9114-9121.

17. W. Niu, L. Zhang and G. Xu, *ACS Nano*, 2010, 4, 1987-1996.

18. Y. Xiong, J. M. McLellan, Y. Yin and Y. Xia, *Angew. Chem., Int. Ed.*, 2007, 46, 790-794.

19. M. Liu, Y. Zheng, L. Zhang, L. Guo and Y. Xia, *J. Am. Chem. Soc.*, 2013, 135, 11752-11755.

20. Y. Wang, H.-C. Peng, J. Liu, C. Z. Huang and Y. Xia, *Nano Lett.*, 2015, 15, 1445-1450.

21. B. Lim, Y. Xiong and Y. Xia, *Angew. Chem., Int. Ed.*, 2007, 46, 9279-9282.

22. J. W. Hong, S. W. Kang, B.-S. Choi, D. Kim, S. B. Lee and S. W. Han, *ACS Nano*, 2012, 6, 2410-2419.

23. H. Zhang, W. Li, M. Jin, J. Zeng, T. Yu, D. Yang and Y. Xia, *Nano Lett.*, 2011, 11, 898-903.

24. C. Zhu, J. Zeng, J. Tao, M. C. Johnson, I. Schmidt-Krey, L. Blubaugh, Y. Zhu, Z. Gu and Y. Xia, *J. Am. Chem. Soc.*, 2012, 134, 15822-15831.

25. B. T. Sneed, C.-H. Kuo, C. N. Brodsky and C.-K. Tsung, *J. Am. Chem. Soc.*, 2012, 134, 18417-18426.

26. Y. Xia, Y. Xiong, B. Lim and S. E. Skrabalak, *Angew. Chem., Int. Ed.*, 2009, 48, 60-103.

27. H. Zhang, M. Jin, Y. Xiong, B. Lim and Y. Xia, *Acc. Chem. Res.*, 2013, 46, 1783-1794.

28. B. Lim, M. Jiang, J. Tao, P. H. C. Camargo, Y. Zhu and Y. Xia, *Adv. Funct. Mater.*, 2009,

RSC Advances Accepted Manuscript

19, 189-200.

29. Z. Shao, W. Zhu, H. Wang, Q. Yang, S. Yang, X. Liu and G. Wang, *J. Phys. Chem. C*, 2013, 117, 14289-14294.

30. V. K. Lamer and R. H. Dinegar, *J. Am. Chem. Soc.*, 1950, 72, 4847-4854.

31. H.-G. Liao, D. Zherebetskyy, H. Xin, C. Czarnik, P. Ercius, H. Elmlund, M. Pan, L.-W. Wang and H. Zheng, *Science*, 2014, 345, 916-919.

32. Y. Jiang, G. Zhu, F. Lin, H. Zhang, C. Jin, J. Yuan, D. Yang and Z. Zhang, *Nano Lett.*, 2014, 14, 3761-3765.

33. N. K. Geitner, A. Doepke, M. A. Fickenscher, J. M. Yarrison-Rice, W. R. Heineman, H. E. Jackson and L. M. Smith, *Nanotechnology*, 2011, 22, 275607.

34. X. Qi, T. Balankura, Y. Zhou and K. A. Fichthorn, *Nano Lett.*, 2015, 15, 7711-7717.

35. H.-C. Peng, S. Xie, J. Park, X. Xia and Y. Xia, *J. Am. Chem. Soc.*, 2013, 135, 3780-3783.

36. L. Elding, *Inorg. Chim. Acta*, 1972, 6, 683-688.

37. L. Elding, *Inorg. Chim. Acta*, 1972, 6, 647-651.

38. H. Borsook and G. Keighley, *Proc. Natl. Acad. Sci. U. S. A.*, 1933, 19, 875-878.

39. M. Jin, H. Zhang, Z. Xie and Y. Xia, *Angew. Chem., Int. Ed.*, 2011, 50, 7850-7854.

40. R. Shannon, *Acta Crystallographica Section A*, 1976, 32, 751-767.

41. X. Xia, S. Xie, M. Liu, H.-C. Peng, N. Lu, J. Wang, M. J. Kim and Y. Xia, *Proc. Natl. Acad. Sci. U. S. A.*, 2013, 110, 6669-6673.

RSC Advances Accepted Manuscript

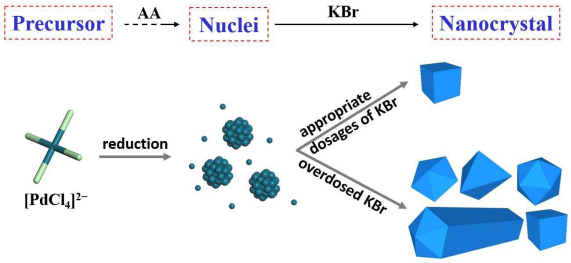

The influence of KBr dosages on the growth pattern of Pd nanocubes.

RSC Advances Accepted Manuscript